OPTIMIZATION OF WIDEBAND FIXED BEAMFORMERS WITH ADAPTIVE SENSOR CALIBRATION

Gerhard Doblinger

Institute of Communications and Radio-Frequency Engineering
Vienna University of Technology
Gusshausstr. 25/389, A-1040 Vienna, Austria
phone: + (43) 1 58801 38927, fax: + (43) 1 58801 38999, email: gerhard.doblinger@tuwien.ac.at,
web: www.nt.tuwien.ac.at/staff/gerhard-doblinger/

ABSTRACT

In this paper, we present optimization methods based on second-order cone programming (SOCP) for wideband beamforming arrays. A serious problem in the design of wideband beamformers with optimized beam patterns is the sensitivity in regard to sensor mismatch, sensor noise, and sensor position errors. Especially in case of beam patterns with high sidelobe attenuation, standard methods like limiting the beamformer coefficient vector norm, or diagonal loading of the sensor correlation matrix are not sufficient to deal with sensor mismatch. Therefore, we use an adaptive calibration of the array sensors. The adaptive calibration filters are trained during a setup phase, and use the same filter structures as the fixed beamformer. After calibration, the filter coefficients are convolved with the optimized beamformer coefficients. Experimental results show the improved performance of arrays with microphones having rather large sensor tolerances.

1. INTRODUCTION

Wideband beamforming arrays have many applications including microphone arrays in the audio frequency range, and beamformers for wideband wireless systems. The optimization criteria for such systems may be different but most applications demand for a good beamforming behavior, and an insensitivity against sensor mismatch, and sensor noise. The latter properties are particularly needed in case of microphone arrays which normally use mismatched sensors. Therefore, a robust design is inevitable, and sensor errors must be considered to obtain a benefit from the beamformer optimization.

There are several well known methods of robust beamformer design [1]. However, these methods are not always sufficient to implement optimized beamformers with mismatched sensors. At least in case of microphone arrays with off-the-shelf sensors, a sensor calibration should be used. For this purpose, we apply a straight forward procedure as proposed in [2, 3].

Optimization of beamforming arrays using SOCP has been studied in [4, 5, 6, 7]. In case of wideband arrays, the mainlobe and sidelobe regions of the beam pattern are optimized within a range of source directions, and within a frequency band. The very large amount of constraints, however, may be prohibitive to find a feasible solution of the optimization problem. Therefore, we propose to eliminate the frequency dependence by optimization of the wideband beam pattern instead. The wideband beam pattern shows the dependence of the beamformer output on the direction of a wideband source signal. With this approach, the computational demand is significantly reduced. In addition, an optimized design of 2- and 3-dimensional arrays with an increased number of sensors is also feasible.

In section 2, we derive a framework for SOCP-based optimization of linearly constrained minimum variance (LCMV), and of weighted least squares (WLS) wideband beamformers. Section 3 gives a brief description of the adaptive system used for automatic sensor calibration. Some representative experimental results are discussed in section 4, followed by a conclusion in Section 5.

2. FILTER-AND-SUM BEAMFORMER

Wideband beamformers may be implemented by processing each sensor signal with optimized finite impulse response duration (FIR) filters as shown in Fig. 1.

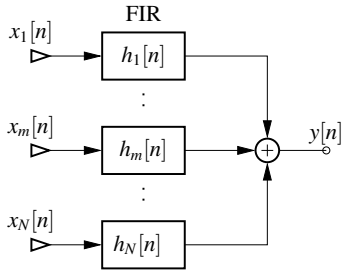

Figure 1: Filter-and-sum beamformer using FIR filters with real-valued impulse responses $h_m[n]$.

The beamformer output signal spectrum using filters with length L real-valued impulse responses $h_m[n]$, $m = 1,2,\ldots,N$ is given by

$$\begin{aligned} Y(e^{j\theta}) &= \sum_{m=1}^{N} H_m(e^{j\theta}) X_m(e^{j\theta}) \\ &= \sum_{m=1}^{N} \underbrace{\sum_{n=0}^{L-1} h_m[n]\, e^{-j\theta n}}_{H_m(e^{j\theta})} X_m(e^{j\theta}), \end{aligned} \tag{1}$$

with FIR filter frequency responses $H_m(e^{j\theta})$, and sensor signal spectra $X_m(e^{j\theta})$ (frequency variable $\theta = \frac{2\pi f}{f_s}$, and sam-

 ISSN 2076-1465

pling frequency f_s). In the sequel, we will derive the beamformer output power needed in the optimization cost function. We stack all real-valued impulse response vectors $\mathbf{h}_m = [h_m[0], \ldots, h_m[L-1]]^T$, $m = 1, \ldots, N$ to the $NL \times 1$ vector $\mathbf{h} = [\mathbf{h}_1, \ldots, \mathbf{h}_N]^T$ which must be found by the design procedures. In addition, the sensor signal spectra are combined to $N \times 1$ vector $\mathbf{x}(e^{j\theta}) = [X_1(e^{j\theta}), \ldots, X_N(e^{j\theta})]^T$. Applying this vector notation, the beamformer output signal spectrum in (1) can be expressed by

$$Y(e^{j\theta}) = \underbrace{\mathbf{x}^T(e^{j\theta})\left(\mathbf{I} \otimes \mathbf{e}^T(e^{j\theta})\right)}_{\mathbf{a}^H(e^{j\theta})} \mathbf{h} = \mathbf{a}^H(e^{j\theta})\,\mathbf{h}. \quad (2)$$

$\mathbf{I}$ is the $N \times N$ identity matrix, $\otimes$ represents the Kronecker product, ^{H} denotes conjugate transpose, and $L \times 1$ vector $\mathbf{e}$ is defined by

$$\mathbf{e}(e^{j\theta}) = [1, e^{-j\theta}, e^{-j2\theta}, \ldots, e^{-j(L-1)\theta}]^T. \quad (3)$$

Using (2) with real-valued $\mathbf{h}$ and $(\mathbf{A} \otimes \mathbf{B})^T = \mathbf{A}^T \otimes \mathbf{B}^T$, the power spectral density (PSD) of the beamformer output signal results in

$$\begin{aligned} S_y(\theta) &= E\left\{Y(e^{j\theta})Y^*(e^{j\theta})\right\} \\ &= \mathbf{h}^T\left(\mathbf{I} \otimes \mathbf{e}(e^{j\theta})\right)\mathbf{S}_{\mathbf{xx}}(\theta)\left(\mathbf{I} \otimes \mathbf{e}^H(e^{j\theta})\right)\mathbf{h}. \end{aligned} \quad (4)$$

$\mathbf{S}_{\mathbf{xx}}(\theta) = E\{\mathbf{x}(e^{j\theta})\mathbf{x}^H(e^{j\theta})\}$ is the $N \times N$ sensor signal spectral correlation matrix, and $E\{\cdot\}$ denotes expectation operation. Applying $\mathbf{S}_{\mathbf{xx}}(\mathbf{I} \otimes \mathbf{e}^H) = \mathbf{S}_{\mathbf{xx}} \otimes \mathbf{e}^H$ (note the dimensions of $\mathbf{S}_{\mathbf{xx}}$, $\mathbf{I}$, $\mathbf{e}$), and the Kronecker product property $(\mathbf{A} \otimes \mathbf{B})(\mathbf{C} \otimes \mathbf{D}) = \mathbf{AC} \otimes \mathbf{BD}$, we finally get the PSD

$$S_y(\theta) = \mathbf{h}^T\left(\mathbf{S}_{\mathbf{xx}}(\theta) \otimes \mathbf{e}(e^{j\theta})\mathbf{e}^H(e^{j\theta})\right)\mathbf{h}. \quad (5)$$

The output signal power of a wideband beamformer operating in a frequency band $\theta \in [\theta_l, \theta_u]$ is given by

$$\begin{aligned} P_y &= \frac{1}{2\pi}\int_{\theta_l}^{\theta_u} S_y(\theta)d\theta + \frac{1}{2\pi}\int_{-\theta_u}^{-\theta_l} S_y(\theta)d\theta \\ &= \mathbf{h}^T \underbrace{\frac{1}{\pi}\int_{\theta_l}^{\theta_u} \Re e\left\{\mathbf{S}_{\mathbf{xx}}(\theta) \otimes \mathbf{e}(e^{j\theta})\mathbf{e}^H(e^{j\theta})\right\} d\theta}_{\mathbf{R}_{\mathbf{xx}}}\,\mathbf{h} \\ &= \mathbf{h}^T\mathbf{R}_{\mathbf{xx}}\,\mathbf{h}. \end{aligned} \quad (6)$$

The $NL \times NL$ correlation matrix $\mathbf{R}_{\mathbf{xx}}$ in (6) can be evaluated in closed form for some types of sensor signal models like uncorrelated sensor noise, diffuse noise fields, and directional noise fields (jammers). However, in most practical situations we must approximate the integral in $\mathbf{R}_{\mathbf{xx}}$ by a sum using a set of different frequencies θ_k, $k = 1, \ldots, N_f$ in the desired frequency band $[\theta_l, \theta_u]$:

$$\mathbf{R}_{\mathbf{xx}} \approx \frac{1}{N_f}\sum_{\theta_k \in [\theta_l, \theta_u]} \Re e\left\{\mathbf{S}_{\mathbf{xx}}(\theta_k) \otimes \mathbf{e}(e^{j\theta_k})\mathbf{e}^H(e^{j\theta_k})\right\}. \quad (7)$$

The standard optimization of a beamformer is based on the minimization of the output signal power from all directions under the constraint that signals from the desired direction (look direction) are maintained. Additional constraints may be imposed regarding sidelobe attenuation, sensitivity to uncorrelated sensor noise, and sensor position errors. The input spectral correlation matrix $\mathbf{S}_{\mathbf{xx}}$ (and $\mathbf{R}_{\mathbf{xx}}$, respectively) must be known in order to solve these optimization problems. If we do not estimate $\mathbf{S}_{\mathbf{xx}}$ adaptively or prior to the beamforming process, we can use the following model in (7):

$$\begin{aligned} \mathbf{S}_{\mathbf{xx}}(\theta) &= \mathbf{S}_d(\theta) + \mathbf{S}_n(\theta) + \mathbf{S}_{\text{diff}}(\theta) + \mathbf{S}_i(\theta) \\ &= S_d(\theta)\mathbf{d}_d(e^{j\theta})\mathbf{d}_d^H(e^{j\theta}) + \sigma_n^2\mathbf{I} + \mathbf{S}_{\text{diff}}(\theta) \\ &\quad + \sum_{k=1}^{I}\sigma_k^2\mathbf{d}_k(e^{j\theta})\mathbf{d}_k^H(e^{j\theta}). \end{aligned} \quad (8)$$

In this model, $\mathbf{S}_{\mathbf{xx}}$ is composed of the spectral correlation matrix $\mathbf{S}_d$ of the signal (with spectrum $S_d(\theta)$) from the desired direction, the spectral correlation matrix $\mathbf{S}_n$ of uncorrelated sensor noise, a diffuse noise field component $\mathbf{S}_{\text{diff}}$, and the contribution of unwanted interferences (jammers). The $\mathbf{d}$-vectors in (8) depend on the wave field model used to describe propagation of the desired signal, and the jammer signals, respectively. Without knowledge of the actual wave propagation, we may assume plane waves traveling towards the array. The sensor signals are then delayed versions of the source signals. In that case, the $\mathbf{d}_d$-vector in (8) is given by

$$\mathbf{d}_d(e^{j\theta}) = \left[e^{j\theta\tau_1(\phi_d)}, \ldots, e^{j\theta\tau_N(\phi_d)}\right]^T, \quad (9)$$

with desired direction ϕ_d. A similar equation holds for $\mathbf{d}_k$ of the k jammer directions in (8). The signal delays τ_m depend on the array layout. In case of a one-dimensional array with sensors aligned on the x-axis, the delays are $\tau_m(\phi) = \frac{f_s}{c}x_m\cos\phi$, $m = 1, \ldots, N$, (sampling frequency f_s, speed of propagation c, x-coordinates x_m, and azimuth ϕ).

In the following, we will need the beamformer output spectrum for the desired wideband source signal. Using $S_d(\theta) \equiv 1$ and (2), we get $Y_d(e^{j\theta}) = \mathbf{a}_d^H(e^{j\theta})\,\mathbf{h}$ with

$$\mathbf{a}_d^H(e^{j\theta}) = \mathbf{d}_d^T(e^{j\theta})\left(\mathbf{I} \otimes \mathbf{e}^T(e^{j\theta})\right). \quad (10)$$

($N \times N$ identity matrix $\mathbf{I}$, and vector $\mathbf{e}$ defined in (3)).

2.1 LCMV beamformer design with sidelobe constraints

A beamformer design with an LCMV criterion is based on the minimization of the beamformer output signal power P_y subject to linear constraints regarding the beamformer responses in certain directions. A special case of an LCMV design is a minimum variance distortionless response (MVDR) beamformer which uses only one desired direction constraint. The optimization problem of an LCMV design can be expressed with (6) by

$$\mathbf{h} = \arg\min_{\mathbf{h}} \mathbf{h}^T\mathbf{R}_{\mathbf{xx}}\,\mathbf{h} \quad \text{subject to} \quad \mathbf{C}^T\mathbf{h} = \mathbf{f}. \quad (11)$$

The constraints $\mathbf{C}^T\mathbf{h} = \mathbf{f}$ guarantee a distortionless response in desired direction. In addition, we can include constraints for spatial nulls in certain directions. As an alternative, however, the minimization of $\mathbf{h}^T\mathbf{R}_{\mathbf{xx}}\,\mathbf{h}$ also gives rise to spatial nulls, if we include jammer terms in the spectral correlation matrix (see (8)). Therefore, we take into account only desired response constraints in (11). Since signals from the desired

direction are not to be distorted by the beamformer, the desired response must be a signal delay for these signals:

$$Y_d(e^{j\theta}) = \mathbf{a}_d^H(e^{j\theta})\,\mathbf{h} = e^{-j\theta\frac{L-1}{2}}, \quad \forall\theta \in [\theta_l, \theta_u]. \qquad (12)$$

The delay of the desired signal is set to $\frac{L-1}{2}$ (FIR filter length L) in order to avoid non-causal filters. Splitting (12) in real and imaginary parts at N_f different frequencies $\theta_k \in [\theta_l, \theta_u]$, the constraints in (11) can be rewritten as

$$\underbrace{\begin{bmatrix} \Re e\{\mathbf{a}_d^H(e^{j\theta_1})\} \\ \vdots \\ \Re e\{\mathbf{a}_d^H(e^{j\theta_{N_f}})\} \\ \Im m\{\mathbf{a}_d^H(e^{j\theta_1})\} \\ \vdots \\ \Im m\{\mathbf{a}_d^H(e^{j\theta_{N_f}})\} \end{bmatrix}}_{\mathbf{A}_d} \mathbf{h} = \underbrace{\begin{bmatrix} \cos\theta_1 \frac{L-1}{2} \\ \vdots \\ \cos\theta_{N_f} \frac{L-1}{2} \\ -\sin\theta_1 \frac{L-1}{2} \\ \vdots \\ -\sin\theta_{N_f} \frac{L-1}{2} \end{bmatrix}}_{\mathbf{b}_d}. \qquad (13)$$

Using the method of Lagrange multipliers, the solution of the optimization problem in (11) is

$$\mathbf{h} = \mathbf{R}_{\mathbf{xx}}^{-1}\mathbf{C}\left(\mathbf{C}^T\mathbf{R}_{\mathbf{xx}}^{-1}\mathbf{C}\right)^{-1}\mathbf{f}, \qquad (14)$$

with $\mathbf{C}^T = \mathbf{A}_d$, and $\mathbf{f} = \mathbf{b}_d$.

With a wideband LCMV beamformer design, we have only a limited control on the mainlobe, and on the sidelobe behavior. Besides the obvious influence of array layout and number of sensors, the directivity of the array pattern can be improved to a certain extend by fine-tuning the diagonal loading of correlation matrix $\mathbf{R}_{\mathbf{xx}}$.

Improved array patterns are obtained with numerical optimization techniques. By "improved" we mean that a smaller mainlobe width, and/or a better sidelobe attenuation can be achieved as compared to an LCMV design with the same array layout. The obvious method to improve the LCMV design is to include constraints on the sidelobe levels [5, 6]. This results in the following optimization problem:

$$\mathbf{h} = \arg\min_{\mathbf{h}} \mathbf{h}^T\mathbf{R}_{\mathbf{xx}}\mathbf{h} \qquad (15)$$

$$\text{subject to} \quad \mathbf{A}_d\mathbf{h} = \mathbf{b}_d \qquad (16)$$

$$\left|\mathbf{a}_{\phi_j}^H(e^{j\theta_i})\mathbf{h}\right| \le \varepsilon_i, \quad \phi_j \in \text{SLR}, \quad j = 1,2,\ldots,N_{\phi_s}, \qquad (17)$$

where $i = 1,2,\ldots,N_f$ is the frequency index, and SLR denotes the side lobe regions of the desired beam pattern. The sidelobe constraints (17) are given for N_f frequency points in $[\theta_l, \theta_u]$, and for N_{ϕ_s} directions in SLR. Vector $\mathbf{a}_{\phi_j}(e^{j\theta_i})$ is defined similar to $\mathbf{a}_d(e^{j\theta_i})$ in (10). Since wideband beamformers like microphone arrays operate over a large frequency band, the number of sidelobe constraints may be prohibitive to obtain a feasible optimization problem. In order to alleviate this problem, we eliminate the frequency dependence of the sidelobe constraints (17) by optimizing the wideband beam pattern within the SLR. The wideband beam pattern represents the beamformer output as a function of the direction of a wideband source signal. We can now reformulate the optimization problem as follows:

$$\mathbf{h} = \arg\min_{\mathbf{h}} \mathbf{h}^T\mathbf{R}_{\mathbf{xx}}\mathbf{h} \qquad (18)$$

$$\text{subject to} \quad \mathbf{A}_d\mathbf{h} = \mathbf{b}_d \qquad (19)$$

$$\left\|\mathbf{A}_{\phi_j}\mathbf{h}\right\| \le \varepsilon, \quad \phi_j \in \text{SLR}, \quad j = 1,2,\ldots,N_{\phi_s}, \qquad (20)$$

where $\|\cdot\|$ is the Euclidean norm, and $N_f \times NL$ matrix $\mathbf{A}_{\phi_j}$ is given by

$$\mathbf{A}_{\phi_j} = \begin{bmatrix} \mathbf{a}_{\phi_j}^H(e^{j\theta_1}) \\ \vdots \\ \mathbf{a}_{\phi_j}^H(e^{j\theta_{N_f}}) \end{bmatrix}. \qquad (21)$$

This optimization problem can be easily transformed to an SOCP problem [8, 9, 10]. Implementation details of the optimization problem are documented in a MATLAB program available at the author's homepage. Nevertheless, the following modifications of the optimization problem are useful in practice:

1. The sensitivity of a beamformer design in regard to white sensor noise may be significantly reduced by limiting the beamformer white noise gain. This gain is approximately determined by the norm of $\mathbf{h}$ (see (6) with $\mathbf{S}_{\mathbf{xx}} = \sigma_n^2\mathbf{I}$). Thus, an additional constraint $\|\mathbf{h}\| \le \varepsilon_h$ should be used in the optimization problem.
2. The mainlobe width of a wideband beamformer is normally larger at the low frequency end. As a consequence, the sidelobe regions in a 3-dimensional beam pattern are increasing with frequency. In principle, a wideband LCMV beamformer with frequency independent mainlobe widths may be designed by increasing superdirectivity at lower frequencies. This can be achieved with a frequency dependent diagonal loading of $\mathbf{S}_{\mathbf{xx}}$. However, such a beamformer is less robust against sensor noise. Consequently, frequency dependent sidelobe regions for the computation of $\mathbf{A}_{\phi_j}$ in (21) should be used to reduce the beamformer white noise gain.

2.2 Weighted least-squares beamformer design with sidelobe constraints

Beamformers based on an LCMV design offer a sharp mainlobe. This property is convenient, if the desired direction is fixed, i.e. there are no substantial movements of the source. In many situations, however, a broader mainlobe is desirable to avoid a significant performance loss is case of look direction mismatch. In such cases, the beamformer design may be based on the approximation of a desired beam pattern similar to the approximation of a spectral mask in an FIR filter design. A well known technique is a weighted least-squares (WLS) design which minimizes the following cost function [7]:

$$J(\mathbf{h}) = \sum_{n=1}^{N_\phi}\sum_{k=1}^{N_f} F_{nk}\left|Y_{nk}(\mathbf{h}) - D_{nk}\right|^2, \qquad (22)$$

with real-valued FIR filter coefficient vector $\mathbf{h}$, and sets of N_ϕ directions, and N_f frequencies. The desired response over these sets is denoted by D_{nk}, and the actual beamformer response is given by $Y_{nk}(\mathbf{h}) = \mathbf{a}_n^H(e^{j\theta_k})\mathbf{h} = \mathbf{a}_{nk}^H\mathbf{h}$ in accordance to (2). Weights F_{nk} may be used to emphasize mainlobe or sidelobe behavior. Expanding the squared magnitude in (22), and using the abbreviations

$$\mathbf{R} = \sum_{n=1}^{N_\phi}\sum_{k=1}^{N_f} F_{nk}\,\Re e\left\{\mathbf{a}_{nk}\mathbf{a}_{nk}^H\right\} \qquad (23)$$

$$\mathbf{q} = \sum_{n=1}^{N_\phi}\sum_{k=1}^{N_f} F_{nk}\,\Re e\left\{D_{nk}\mathbf{a}_{nk}\right\} \qquad (24)$$

results in

$$J(\mathbf{h}) = \mathbf{h}^T \mathbf{R}\,\mathbf{h} - 2\,\mathbf{q}^T \mathbf{h} + \text{constant}. \tag{25}$$

Setting the gradient $\nabla_{\mathbf{h}} J$ to zero in order to minimize $J(\mathbf{h})$ yields

$$\mathbf{h} = \mathbf{R}^{-1}\mathbf{q}, \tag{26}$$

provided that $\mathbf{R}$ is invertible. The WLS design method is extended in [7] by iterative procedures to obtain robust beamformers. As a computationally more efficient alternative, we propose the following constrained optimization problem which can easily be solved by SOCP:

$$\mathbf{h} = \arg\min_{\mathbf{h}} \; \mathbf{h}^T \mathbf{R}\,\mathbf{h} - 2\,\mathbf{q}^T \mathbf{h} \tag{27}$$

$$\text{subject to} \quad \left\|\mathbf{A}_{\phi_j}\mathbf{h}\right\| \le \varepsilon, \quad \phi_j \in \text{SLR} \tag{28}$$

$$\|\mathbf{h}\| \le \varepsilon_h. \tag{29}$$

As mentioned in the previous section, we also include a norm constraint on the FIR filter coefficient vector $\mathbf{h}$ to limit the beamformer white noise gain. Further details can be found in a MATLAB program available at the author's home page.

3. ADAPTIVE SENSOR CALIBRATION

Optimized wideband beamformers are quite sensitive to a mismatch in sensor transfer functions. In case of microphone arrays, this means that we must use preselected sensors, or some calibration procedure. A rather effective automatic calibration can be implemented with an adaptive filter in each sensor channel [2, 3]. These filters compensate sensor tolerances by matching sensor transfer functions prior to normal use of the array. We assume omnidirectional microphones with no angle-dependent errors in the polar patterns. Such errors cannot be compensated by the adaptive system we use in cascade to the beamformer.

In the calibration phase, the array is exposed to a wideband signal like speech or noise coming from broad side. The only requirement is an equal excitation of all sensors. After the calibration phase, the beamformer FIR filter coefficients are convolved with the final coefficients of the adaptive filters. During normal operation, there is no computational overhead due to calibration.

The block diagram of the adaptive sensor calibration system is shown in Fig. 2. The system is connected between the sensor outputs $s_m[n]$ and the beamformer inputs $x_m[n]$.

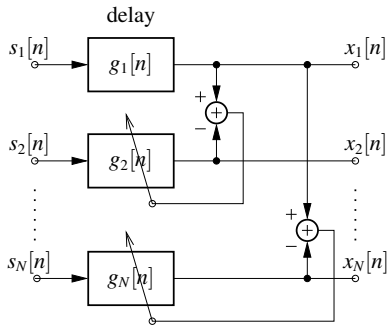

Figure 2: Adaptive filters for sensor calibration (channel 1 is used as reference, $g_m[n], m = 2,\ldots,N$ are the filter impulse responses after convergence).

Sensor channel 1 serves as a reference channel. Note that impulse response $g_1[n] = \delta[n - N_d]$ represents a signal delay by N_d samples in order to ensure causal adaptive filters. After convergence of the adaptive filters, the filter coefficients are kept constant to get the transfer functions

$$G_m(e^{j\theta}) = \frac{X_m(e^{j\theta})}{S_m(e^{j\theta})} = \frac{H_1(e^{j\theta})\,e^{-j\theta N_d}}{H_m(e^{j\theta})}, \quad m = 2,\ldots,N, \tag{30}$$

where $H_m(e^{j\theta})$ are the sensor transfer functions. As already mentioned, all sensors are exposed to the same calibration signal $s_c[n]$. Therefore, the sensor spectra to be used in (30) are $S_m(e^{j\theta}) = H_m(e^{j\theta})S_c(e^{j\theta})$. As indicated in (30), the sensor transfer functions must be invertible, and thus must have strict minimum phase. Our experiments show that in case of microphone arrays, sufficient convergence is obtained with adaptive FIR filters using the normalized least mean squares (NLMS) algorithm.

4. EXPERIMENTAL RESULTS

In this section, we present representative examples of wideband beamformer designs. The design data used are suitable for microphone array beamformers. However, other applications can be implemented by scaling frequencies, array layout, and wave propagation model. The relative bandwidth of microphone arrays is approximately a factor 2, and is much larger than that of wideband arrays operating at sonar or radio frequencies. As a consequence, microphone arrays are a special challenge for wideband beamformer designs.

The results are given for 1-dimensional, linear, uniform arrays with $N = 8$ sensors, and a look direction of 0° (endfire). Extensions to other array configurations are straight forward since the only modification of the design equations concerns the $\mathbf{d}$ vector in (9). We use a frequency band from 400 Hz up to 3200 Hz, with 8 kHz sampling frequency. Sensor spacing is 5 cm giving rise to an array size of 35 cm. Typically, the FIR filter length of both the beamformer, and the adaptive calibration filters is set to $L = 50$.

In order to investigate the influence of sensor errors, we model microphone frequency responses by 4^{th}-order recursive filters approximating a typical magnitude response with a 6 dB decay below 700 Hz, and a 2 dB increase around 3 kHz. This response is randomly disturbed by small deviations to obtain maximum amplitude and phase errors of approximately 2 dB, and 10°, respectively. The exact shape of the microphone frequency response is not important for adaptive sensor calibration, as long as no deep notches or steep slopes are present.

A result of an LCMV design improved by SOCP is shown in Fig. 3. The beam pattern is obtained after a calibration time period of 250 msec. using a wideband noise signal common to all sensors. In addition, sensor noise (SNR = 30 dB) is included to show the wide noise behavior of the beamformer. Ten different sets of sensors are used to obtain the beam patterns. The patterns of the arrays with calibrated sensors approximate the optimized pattern quite well. However, the desired spatial null at 90° is barely visible. We observe this property at nearly all fixed beamformer designs with real sensors. The effect of using non-calibrated sensors is demonstrated in Fig. 4. According to our experiments with different design setups, it is nearly impossible to obtain a benefit from sidelobe optimization without using calibrated sensors.

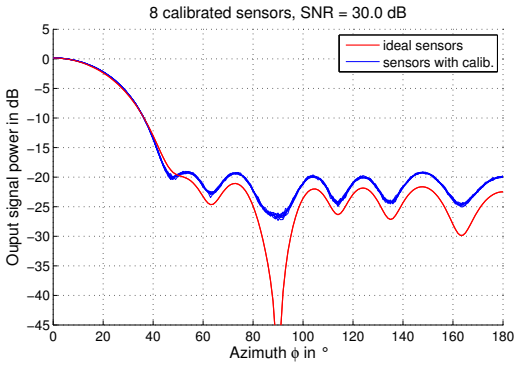

Figure 3: Wideband beam patterns of $N = 8$ calibrated uniform arrays (LCMV+SOCP design).

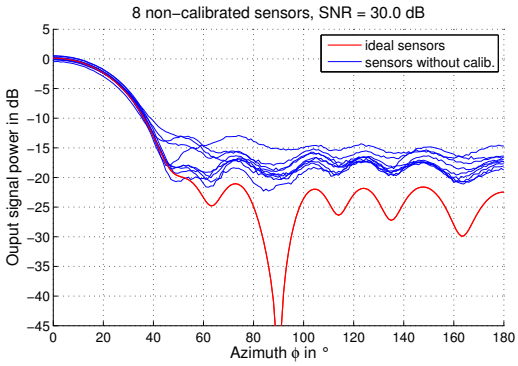

Figure 4: Wideband beam patterns of $N = 8$ non-calibrated uniform arrays (LCMV+SOCP design).

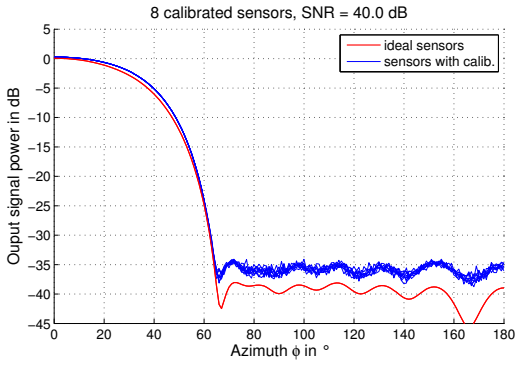

Figure 5: Wideband beam patterns of $N = 8$ calibrated uniform arrays (WLS+SOCP design).

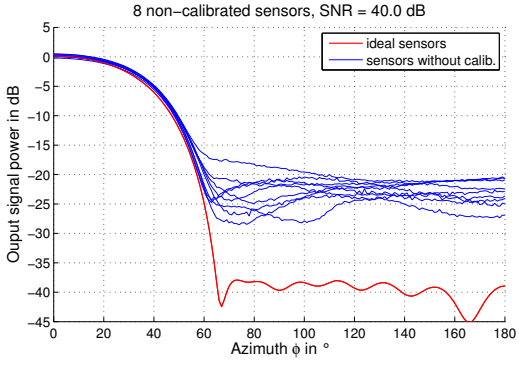

Figure 6: Wideband beam patterns of $N = 8$ non-calibrated uniform arrays (WLS+SOCP design).

A design result using the SOCP in (27)-(29) is shown in Fig. 5 in case of arrays with adaptive sensor calibration. Compared to Fig. 3, we obtain a flat mainlobe, and a much higher sidelobe attenuation. However, arrays designed by this method are more sensitive to uncorrelated sensor noise. In addition, they are also more sensitive regarding mismatch of sensor transfer functions (see Fig. 6).

More experimental results including the 3-dimensional beam patterns of the examples can be found on the author's home page.

5. CONCLUSIONS

We have presented optimized design methods for wideband beamformers based on SOCP. By approximating the wideband beam pattern directly, our approach offers a lower computational complexity as compared to other methods. In order to obtain an improved sidelobe behavior with mismatched sensors, we promote the use of an adaptive sensor calibration scheme. Experiments show that the resulting beam patterns are close to the optimized patterns of arrays with ideal sensors.

REFERENCES

[1] J. Li, P. Stoica, (Eds.), "Robust adaptive beamforming," John Wiley & Sons. Inc., 2006.

[2] D. Van Compernolle, "Switching adaptive filters for enhancing noisy and reverberant speech from microphone array recordings," , *Proc. IEEE Int. Conf. Acoustics, Speech, Signal Processing*, vol. 2, pp. 833-836, April 1990.

[3] M. Buck, T. Haulick, H.-J. Pfeiderer, "Self-calibrating microphone arrays for speech signal acquisition: a systematic approach," *Signal Processing*, vol. 86, pp. 1230-1238, 2006.

[4] H. Lebret, S. Boyd, "Antenna array pattern synthesis via convex optimization," *IEEE Trans. Signal Processing*, vol. 45, pp. 526-532, Mar. 1997.

[5] J. Liu, A.B. Gershman, Z.-Q. Luo, K.M. Wong, "Adaptive Beamforming with sidelobe control: a second-order cone programming approach," *IEEE Signal Proc. Letters*, vol. 10. pp. 331-334, Nov. 2003.

[6] S. Yan, C. Hou, and X. Ma, "Convex optimization based time-domain broadband beamforming with sidelobe control," *J. Acoust. Soc. Am.*, vol. 124, pp. 46-49, Jan. 2007.

[7] H. Chen, W. Ser, "Design of robust broadband beamformers with passband shaping characteristics using Tikhonov regularization," *IEEE Trans. Audio, Speech, and Lang. Processing*, vol. 17, pp. 665-681, May 2009.

[8] S. Boyd, L. Vandenberghe, "Convex optimization," Cambridge University Press 2006.

[9] M. S. Lobo, L. Vandenberghe, S. Boyd, H. Lebret, "Applications of second-order cone programming," Linear Algebra and its Applications 284 (1998) 192-228, Elsevier Science 1998.

[10] M. Grant, S. Boyd, "cvx users' guide, version 1.21" `www.stanford.edu/~boyd/cvx/`, May 31, 2010.